Open Access Article

EFFICIENT MEDICAL IMAGE SEGMENTATION USING SQUIRREL SEARCH ALGORITHM BASED FUZZY LEVEL SET METHOD

Dr.E.Gnanamanoharan
Assistant Professor, Department of Electronics and Communication Engineering,
Faculty of Engineering and Technology, Annamalai University.
gnanamanohar@gmail.com

S. Nandhini Devi
Research Scholar, Annamalai University, Chidambaram
sjnandhinidevi@gmail.com

Abstract

Automated segmentation of brain tumors from MRI images can be essential for behavior planning, monitoring in addition to a diagnosis of a different kind of disease. Hence, in this paper Squirrel Search Algorithm-based Fuzzy Level Set Method (SSA-FLS) is designed aimed at brain tumor segmentation. The proposed segmentation process is designed with the combination of the Fuzzy Level Set method (FLS) and Squirrel Search Algorithm (SSA). In the fuzzy level set method, the efficient cluster center is chosen with the assistance of the Squirrel Search Algorithm. Initially, the fuzzy level set method objective function is considered by tumor portion extraction from the MRI images. After that, SSA is utilized to optimize the cluster center and fuzzifier from the clustering method. The projected technique is applied in MATLAB and performances have been assessed. The projected technique is authenticated by performance metrics like Dice similarity coefficient (DSC), Jaccard Similarity Index (JSI), accuracy, sensitivity, and specificity. The projected technique is contrasted with the conventional techniques like Seagull Optimization Algorithm Based Super Pixel Fuzzy Clustering (SOA-SFC) and Chimp Optimization Algorithm Based Type-2 Intuitionistic Fuzzy C-Means Clustering (COA-T2FCM).

Keywords: *brain tumor segmentation, squirrel search algorithm, fuzzy level set method, cluster center, and medical image segmentation.*

抽象的

从 MRI 图像中自动分割脑肿瘤对于行为规划、监测以及诊断不同类型的疾病至关重要。因此，本文针对脑肿瘤分割设计了基于松鼠搜索算法的模糊水平集方法（SSA-FLS）。所提出的分割过程是结合模糊水平集方法（FLS）和松鼠搜索算法（SSA）设计的。在模糊水平集方

Received: October 05, 2021 / Revised: October 31, 2021 / Accepted: November 30, 2021 / Published: December 31, 2021

About the authors：Dr. E. Gnanamanoharan

Corresponding author- *Email: gnanamanohar@gmail.com

法中，借助松鼠搜索算法选择有效的聚类中心。最初，通过从 MRI 图像中提取肿瘤部分来考虑模糊水平集方法的目标函数。之后，利用SSA从聚类方法中优化聚类中心和模糊器。将投影技术应用于 MATLAB 并评估了性能。预测的技术通过骰子相似度系数 (DSC)、Jaccard 相似度指数 (JSI)、准确性、敏感性和特异性等性能指标进行验证。该投影技术与基于海鸥优化算法的超像素模糊聚类 (SOA-SFC) 和基于黑猩猩优化算法的 Type-2 直觉模糊 C 均值聚类 (COA-T2FCM) 等传统技术进行对比。

关键词：脑肿瘤分割，松鼠搜索算法，模糊水平集方法，聚类中心，医学图像分割。

1. Introduction

In the United States alone, it is computed that 23,000 novel cases of cerebral palsy is analyzed in 2015. Although gliomas can be the most widely recognized mental development, they may be less severe (e.g. poor quality) for a patient in the future for a short time, or stronger (e.g. high quality) for a patient with a maximum of 2 years in the future [1]. Although the medical method for mental cancer is the most popular treatment, radiation in addition to chemotherapy can be utilized to slow the growth. Magnetic resonance imaging (MRI) gives definitive images of the mind, in addition, is one of the most widely recognized tests utilized to identify cerebral cancer [2]. Moreover, the psychiatric cancer segment from the MR images may have an extraordinary effect on further developmental diagnosis, growth rate expectation, and treatment arrangements. Some growths, for example, can effectively differentiate meningiomas, while others are more difficult to control, such as glioblastomas and gliomas [3].

These growths (with their involving edema) are often diffuse, do not differ sufficiently, and they expand into patches-like designs which make it problematic to dissect. An additional important problem with fragmented mental development is that they show any area of the cerebellum [4], which fits into a fiddle in additional size. Besides, different from the images obtained from X-ray computed tomography (CT) scans, the magnitude of the vowel parameters in the MR images is not normalized. The MR engine used (1.5, 3, or 7 Tesla) [5] in addition to the safety conference (vision value, voxel goal, inclination strength, b0 rating, etc.) will have a unique grayscale value when imagined in various emergency clinics. Furthermore, the individual dynamic is one of the basic components of the primary and intelligent structures, especially in the field of medical processing [6]. To get such a structure, it is important to conclude serious investigations of the images. The first and most important improvement is a planned or separate MRI unit image investigation. In these ways, further improving the accuracy of the section of medical images will enhance the exhibition of master and ingenious structures. As a result, a classification of investigations was conducted for the MR image segment [7].

Again, discriminating models are succinctly simple because they rely on low-level image highlights to be obtained from enlightened

production images to accurately capture nearby appearance types [8]. The MRI image segmentation technique to K- means clustering the exhibition with a fuzzy C-means clustering system. Thresholding in addition level set division positions is followed to provide proper cerebral tumor identification. This method can obtain parts of unlimited computational time for the image segment of the K-means group. Similarly, it can obtain the best conditions of ambiguous C-means in precision fragments. The adaptive regulated strip-based MRI image cerebral tumor segment obscure C-marker boxing system had potential gains for adaptation to the local system [9]. It has been updated with the power to reduce image sophistication, the possibility of collection boundaries, and computational costs. However, these techniques do not achieve the best fragmentary effects on the MRI image [10]. Recently, to achieve the best-segmented results in MRI images, the clustering process is utilized with the Artificial Intelligence (AI) techniques such as Grey Wolf Optimization (GWO), Whale Optimization Algorithm (WOA), and Particle Swarm Optimization (PSO). The main contribution and organization of the paper are presented in this section.

Contribution and organization of the research

- ❖ SSA-FLS is designed intended for brain tumor segmentation. The projected segmentation process is designed with the combination of FLS and SSA. In the fuzzy level set method, the efficient cluster center is chosen with the help of the Squirrel Search Algorithm.
- ❖ Initially, the fuzzy level set method objective function is considered by tumor portion extraction from the MRI images. After that, SSA is utilized to optimize the cluster center and fuzzifier from the clustering method.
- ❖ The projected technique is applied in MATLAB in addition performances will be evaluated. The projected technique is authenticated by performance metrics like Jaccard Similarity Index (JSI), Dice similarity coefficient (DSC), accuracy, sensitivity, and specificity.
- ❖ The proposed method is compared with the existing methods such as Seagull Optimization Algorithm Based Super Pixel Fuzzy Clustering (SOA-SFC) and Chimp Optimization Algorithm Based Type-2 Intuitionistic Fuzzy C-Means Clustering (COA-T2FCM).

The residual portion of the paper is prearranged as follows, section 2 provides the detailed review section of brain tumor segmentation. The detailed description of the proposed method is formulated in section 3. The outcomes of the projected technique are presented in section 5. The conclusion part of the paper is formulated in section 6.

2. Related Works

A wide range of techniques is approached for the segmentation of liver tumors and brain tumors. A part of the techniques is analyzed in this section.

Mohammadreza Soltaninejad *et al.,* [11] have developed a 3D super voxel-related learning technique aimed at separating growth in multimedia MRI cerebrum images (conventional MRI in addition DTI). Super voxels were produced using data in a multimodal MRI database. For each Super Vox, the classification of rules that recall the histograms of the text for

the description determines the use of Capor channels with different sizes and directions, and the first request special elements are removed. Those components were maintained in a random forests (RF) classification to order each supervaxel in the growth center, edema, or sound mind tissue. The strategy is rated in two datasets: 1) Clinical Database: 11 Multiple Images of Patients in addition 2) BRATS 2013 Clinical Database: 30 Multiple Images.

Adel Kermi *et al.,* [12] have formulated a fully robotized, rapid, and accurate cerebral development division technique has been introduced that naturally distinguishes entire cancer from the 3D-MRI. The strategy depends on a cross-racial approach, which is a mental balance selection technique and district-wise and range-based segregation strategies. The section cycle consists of three basic stages. First, the product was applied before the film to remove any confusion and remove the mind from the headline. In the next stage, computerized cancer was identified. It depends on the FBB technique using mental balance. The purchase effect involves the planned introduction of a distorted model, thereby eliminating the need to select the base district in which the customer is interested. After a long time, the tertiary center merged with the 3D decomposable model.

Marco Domenico Cirillo *et al.,* [13] have introduced the 3D Volume-to-Volume Generative Advertising Network aimed at Separating Brain Development. Deep and 87.20%, 81.14%, and 78.67% dice marks and 95 percent for the BraTS test after the 95 Volt 2 Vox models for the 6.44mm, 24.36mm, in addition, 18.95mm Hausdorff distances with 10-Grease cross approval.

Mahnoor ali *et al.,* [14] have presented two-division segmentation networks: a 3D CNN and U-Net, resulting in better and more accurate predictions in a critical and direct integration. Both models were independently produced in the BraTS-19 test database and evaluated to provide split maps. The proposed team attained dice scores of 0.750, 0.906, in addition to 0.846, respectively, in the approval package to improve cancer, full growth, and development center, and now perform better than the currently available structural structures.

Abhisha Mano *et al.,* [15] have presented grid-based methods with Weighted Bee Swarm Intelligence and K-means clustering for brain tumor segmentation. This strategy was very compelling because there are explicit functions of image data and authentication to obtain point-to-point and accurate image testing due to half and half composition and expansion. Network-based segment balance generally calculates the calculation time and minimizes the problem. Weighted bee swarm optimization was used to improve segment boundaries to obtain better execution. Various useful sites, for example, cerebrospinal fluid, opaque material, and white matter were separated using the proposed calculation, which would help to think and depict cancer in general. Investigational outcomes show that the projected system improves vulnerability and implementation measures up to a specific investigation. The interpretation of this method was also improved by a factor of 1.5%.

3. Proposed System Model

Brain tumors can be divided into different types such as secondary and primary tumors. Primary brain tumors are generated from the brain cells which secondary tumors are considered into the

brain from different organs. Hence, in this paper Squirrel Search Algorithm-based Fuzzy Level Set Method (SSA-FLS) is designed for brain tumor segmentation. The proposed segmentation process is designed with the combination of the Fuzzy Level Set method (FLS) and Squirrel Search Algorithm (SSA). In the fuzzy level set method, the efficient cluster center is selected with the help of the Squirrel Search Algorithm. Initially, the fuzzy level set method objective function is considered by tumor portion extraction from the MRI images. After that, SSA is utilized to optimize the cluster center and fuzzifier from the clustering method. The complete architecture of the proposed method is illustrated in figure 1.

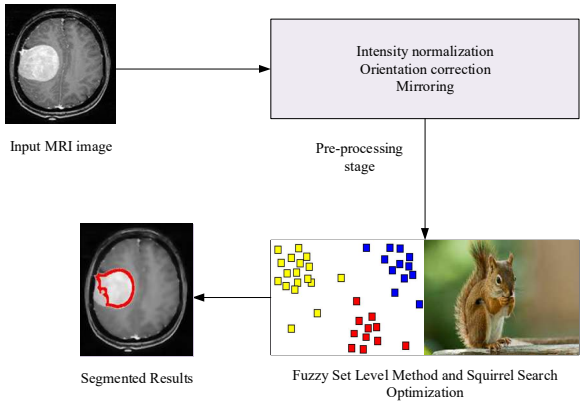

Figure 1: Proposed Architecture

At the initial condition, the dataset is gathered from the open-source system. Afterward, the pre-processing phase is proceeding to eliminate the unwanted noise from the images. The pre-processing image is sent towards the segmentation phase which segments the brain tumor from the MRI images. A detailed description of pre-processing stage and segmentation stage is explained below section.

3.1. Pre-processing phase

In the pre-processing phase, the MRI image unwanted information is removed from the images and improves the quality of the images. The pre-processing methods of the proposed methodology are presented as follows,

(a) intensity normalization

In the brain MRI image, the main disadvantage of the images is the similar kind of tissue does not have an exact intensity. Various MRI arrangements provide various intensity parameters for the similar tissue type smooth within a similar object. These intensity changes give difficult operation of image analysis and segmentation process. Hence, intensity normalization is the required portion in MRI analysis. Here, Gaussian intensity normalization is utilized which rescales the intensity parameters by global linear scaling process. This technique is working by primary strengths alienated through the standard deviation of the complete intensity parameters within one which formulated as follows,

$$I^{new} = \frac{I}{\sigma} \qquad (1)$$

Where σ can be defined as the standard deviation of an entire scan and I can be described as a primary intensity value [16]. Based on this process, the segmentation of the MRI image is achieved in the range of [0,1024], without any important information loss.

(b) Mirroring

Once offset correction and rotation is complete, the image is flipped precipitously towards achieving its mirror-image form. The mirrored one and reference image can be utilized to compare the right and left hemispheres. The pre-

processing step of the MRI image can be eliminating the unsolicited information of the image. After that, the segmentation purpose, the fuzzy level set technique is utilized to segment the brain tumor portions.

3.2. fuzzy level set technique

In this proposed methodology, the FLS technique is utilized to segment the tumor portions from the MRI image. The objective function of the FLS method contains the parameter for the fuzziness index that can be utilized in partitioning. The membership parameter is depending on the cluster center which can be connected to a precise region of interest [17]. The precise region of interest is depending on the particular cluster. The clustering of the objects into a group mostly depends on the objective characteristics. The cluster center is selected with the help of the SSA algorithm. The clusters are computed based on a mean square deviation of different pixels which is presented below,

$$\sigma_{XD} = \sqrt{\left(\sum D\epsilon nx\{D\}\frac{(G` - G)^2}{M-1}\right)} \quad (2)$$

Where, G can be represented as a selected pixel value, $G`$ can be represented as a remaining pixel value. The exponential kernel function is upgraded with the consideration of the above formulations,

$$W_{XD} = Exp\left[-\left(\sigma_{XD} - \frac{\sum_{D\epsilon nx}\sigma_{XD}}{M}\right)\right] \quad (3)$$

After normalization of the computed parameters, the pixel parameters can be upgraded related to larger parameters computed in the neighborhood [18]. Regularization of every pixel parameter can be completed by dividing weight (W) through the sum function of W. Finally, the k means clustering is utilized to categorize the intensity which is presented as follows,

$$F_{R1} = \sum_{I=1}^{N}\int |G(X) - G(C)|U_I(X)dx_{R1} \quad (4)$$

Where, $U_I(X)$ can be described as a region membership function (R1). In the projected clustering, the cluster head is chosen with the assistance of the SSA method which is presented in the below section.

3.2. Squirrel Search Algorithm

To empower the performance of the fuzzy level set, the SSA algorithm is utilized. This algorithm is proceeding with the dynamic foraging method of the moving squirrels and with their locomotion behavior which is named gliding. Flying squirrels can be a distinct flock of arboreal in addition to nocturnal rodents which is incredibly adjusted to slow down. Presently, 15 species in addition to 44 classes of flying squirrels have been recognized, most of which are found in the autumn foothills of Europe in addition to Asia, especially Southeast Asia. The individual endangered class in Eurasia is the Glochomis Volans, also defined as the Southern Flying Squirrel. Flying squirrels look very efficient and modern with a parachute-like layer (Kadakia), that allows the squirrel to skim from one tree to another, in addition, is accomplished of lifting and dragging them. The most intriguing

detail around flying squirrels is which do not fly, but rather they utilize an unusual technique, for example, "skimming" which is considered moderate with interest, allowing creatures with little warm blood to travel long distances efficiently and quickly. In SSA, the search starts with the foraging characteristics of squirrels. The squirrel is searching for food with the consideration of gliding behavior in the warm weather condition. In this scenario, it can change their located place and explore various forests. During the hot climate conditions, its container happens their everyday food requirement very quickly on the diet. The squirrel gets food in a hot climate, it starts to find an optimal food source for winter [19]. The searched foods are stored in a safe place. The stored foods are utilized to enhance the energy in the winter climate in addition decrease the expensive hunting trips, in addition, improve the probability of existence. Some of the assumptions are required to achieve the optimal solutions in SSA which are presented as follows,

- Several squirrels are presented in the forest and expected each squirrel is located in one tree.
- Each flying squirrel independently explorations for food in addition efficiently consumed the obtainable food resources with the consideration of foraging characteristics.
- In a forest, three types of trees can be presented as a hickory tree, oak tree, and normal tree.
- The forest location is considered with two types of trees like one hickory tree and three oak trees.

The SSA initiated with the random placement of flying squirrels which is equal to conventional population-related algorithms. In the SSA, the flying squirrel location can be mentioned as a vector, and dimension search space is mentioned as d. So, the flying squirrels are gliding in 1-D, 2-D, and 3-D or hyperdimensional search space in addition to the variation of their placement vectors.

3.2.1. Initial population

In the initial population, several flying squirrels are initialized as DCNN hyperparameters. Additionally, the flying squirrel location is presented as a vector. The placement of complete flying squirrels is presented as a matrix which is given as follows,

$$L = \begin{bmatrix} L_{1,1} & L_{1,2} & \dots & \dots & L_{1,d} \\ L_{2,1} & L_{2,2} & \dots & \dots & L_{2,1} \\ \dots & \dots & \dots & \dots & \dots \\ \dots & \dots & \dots & \dots & \dots \\ L_{N,1} & L_{N,2} & \dots & \dots & L_{N,d} \end{bmatrix} \quad (5)$$

Here, $L_{i,j}$ can be represented as a jth dimension of ith flying squirrel. The current location of every flying squirrel is allocated with the consideration of normal distribution in the forest.

3.2.2. Fitness Computation

The fitness location of every flying squirrel can be computed with the decision variable values into a user-described fitness function. The fitness function values can be stored in the below array.

$$FF = \begin{bmatrix} F_1([S_{1,1}, S_{1,2}, \dots, S_{1,d}]) \\ F_2([S_{2,1}, S_{2,2}, \dots, S_{2,d}]) \\ \dots \\ \dots \\ F_N([S_{N,1}, S_{N,2}, \dots, S_{N,d}]) \end{bmatrix} \quad (6)$$

The fitness function is mathematically formulated as follows,

$$\mathrm{FF} = \mathrm{MAX}\{\mathrm{PSNR}\} \quad (7)$$

$$PSNR = 10log_{10}\left(\frac{MAX^P}{MSE}\right) \quad (8)$$

$$MSE = \frac{1}{N * M}\sum_{X=1}^{N}\sum_{Y=1}^{M}\left[I_{image}(A,B) - I_{d-image}(A,B)\right]^2 \quad (9)$$

Where, $I_{d-ima}\ (A,B)$ is described as segmented images and $I_{image}(A,B)$ is described as an input image. Based on the fitness function, the DCNN images are selected which are utilized to enhance the optimal semantic segmentation process.

3.2.3. Random selection, declaration, and sorting

Once compute fitness parameters, these parameters are saved in the array. After that, the stored fitness values are arranged in ascending direction. The flying squirrel with minimum fitness parameters can be considered a hickory nut tree. The following three optimal flying squirrels can be measured as the acorn nuts tree which moved near the hickory nut tree. The balance flying squirrels are considered the normal tree. In the flying squirrels, the foraging characteristics are pretentious through the attendance of marauders. This normal character can be changed by considering the location updating technique with the marauder attendance probability function [20].

3.2.4. Generate New locations

The new solutions are generated with the consideration of the dynamic foraging characteristics of flying squirrels. The active foraging characteristics of the flying squirrels with three conditions are mathematically presented in this section.

Condition 1: Flying squirrels are presented in acorn nut trees which moves towards hickory nut trees. The optimal location is computed as follows,

$$S_{AT}^{T+1} = \begin{cases} S_{AT}^{T} + d_g \times g_C \times (S_{HT}^{T} - S_{AT}^{T}) r_1 \geq P_{DP} \\ Random\ location \qquad otherwise \end{cases} \quad (10)$$

Where, S_{HT}^{T} can be described as a location of a flying squirrel in a hickory nut tree, r_1 can be described as a random number, d_g can be described as gliding distance and T can be described as current repetition. The remaining among exploitation in addition exploration can be computed with the consideration of the fixed value of gliding (g_C). The gliding constant value has affected the performance of the proposed technique. This constant value is taken as 1.9 which is computed with the consideration of rigorous analysis.

Condition 2: In this scenario, the flying squirrels are moved to the acorn nut trees to achieve the required food. In this condition, the new location is computed based on the below conditions,

$$S_{NT}^{T+1} = \begin{cases} S_{NT}^{T} + d_g \times g_C \times (S_{AT}^{T} - S_{NT}^{T}) r_2 \geq P_{DP} \\ Random\ location \qquad otherwise \end{cases} \quad (11)$$

Here, the r_2 can be described as an arbitrary parameter in the period [0,1].

Condition 3: In this scenario, the squirrels can be on normal trees which previously spent acorn nuts should move to hickory nut trees to save hickory nuts that are considered at the period of food scarcity. The optimal location of squirrels has achieved tracks,

$$S_{NT}^{T+1} = \begin{cases} S_{NT}^{T} + d_g \times g_C \times (S_{HT}^{T} - S_{NT}^{T}) r_3 \geq P_{DP} \\ Random\ location \qquad otherwise \end{cases} \quad (12)$$

Here, the r_3 can be described as a random parameter in the variety [0,1]. P_{DP} can be described as a probability function taken as 0.1 for three conditions.

3.2.5. Gliding in Aerodynamics

The gliding process of squirrels can be presented with the consideration of equilibrium glide. It is the summation of drag (D) in addition to Lift (L) force and it creates the resultant force (R) whose magnitude is opposite in addition equal to the way which depends on squirrel weight. The lift to drag ratio is presented as follows,

$$\frac{L}{D} = \frac{1}{\tan\theta} \qquad (13)$$

Where θ can be described as glide angle. The flying squirrels can improve their glide path length which increases the drag ratio. The lift outcomes from downward deflection are presented as follows,

$$L = \frac{1}{2\rho c_l v^2 s} \qquad (14)$$

Where s can be described as surface are of body (i.e., 154Cm^2), speed is denoted by $v = 5.25ms^{-1}$, lift coefficient can be denoted as c_l and density of air is denoted as $\rho = 1.204kgm^{-3}$.The frictional drag can be presented as follows,

$$D = \frac{1}{2\rho c_l v^2 s c_d} \qquad (15)$$

Where, c_d can be represented as frictional drag coefficient. In low-speed conditions, the drag parameter can be excessive. Similarly, at high speed, it develops smaller. In the steady-state condition, the glide angle can be computed as follows,

$$\emptyset = arctan\left(\frac{D}{L}\right) \qquad (16)$$

The gliding distance is computed based on the below equation,

$$d_g = \left(\frac{H_g}{\tan\theta}\right) \qquad (17)$$

Where, H_g can be considered as loss in height which is taken as 8m.

3.2.6. Monitoring condition of seasonal

In the SSA, seasonal variation normally disturbs the foraging behaviors of squirrels. It affects heat loss in the condition of very low temperatures. The seasonal constant value should be considered to enhance the performance which presented follows,

$$S_C^T = \sqrt{\sum_{K=1}^{D} \left(S_{AT,K}^{T} - S_{HT,K}^{T}\right)^2} \qquad (18)$$

Where $T = 1,2,3.$

3.2.7. Arbitrary replacement at the close of the winter season

The relocation of the hovering squirrels is designed with the below equation,

$$S_{NT}^{new} = S_L + Levy(N) \times (S_U - S_L) \quad (19)$$

Where the levy can be described as levy distribution function empowers best in addition well-organized search space exploration. Levy distribution function can be presented as shadows,

$$L(S,\gamma,\mu) = \begin{cases} \sqrt{\frac{\gamma}{2\pi}} & \exp\left[-\frac{\gamma}{2(s-\mu)}\right]\frac{1}{(s-\mu)^{3/2}} \\ 0 & otherwise \end{cases} < \mu < s < \infty \quad (20)$$

Where, $\mu, \gamma > 0$, μ can be described shift parameter, γ can be described as the scale parameter. The levy flight can be computed as follows,

$$Levy\ (x) = 0.01 \times \frac{r^a \times \sigma}{|r^b|^{\frac{1}{\beta}}} \quad (21)$$

Here, β can be considered as constant (i.e., 1.5), r^b and r^a can be described as two typically dispersed arbitrary parameters in [0,1].

$$\sigma = \left[\frac{\Gamma(1+\beta) \times sin\left(\frac{\pi\beta}{2}\right)}{\Gamma\left(\frac{1+\beta}{2}\right) \times \beta \times 2^{\left(\frac{\beta-1}{2}\right)}}\right]^{\frac{1}{\beta}} \quad (22)$$

Here, $\Gamma(x) = (x-1)!$

3.2.8. Stopping condition

The final termination condition is a commonly utilized convergence condition in that a allowable but reference parameter can be described among the final two upcoming outcomes. In this condition, extreme iteration can be checked. Based on the algorithm, the optimal fuzzy level set parameter is selected.

4. Results and discussion

The presentation of the projected technique is presented in this section. The projected method is analyzed with the performance metrics. The projected technique can be applied in an Intel Core i5-2450M CPU 2.50GHz laptop and 6GB RAM. The presented technique can be applied in MATLAB software R2016b. To validate the projected methodology, the databases can be collected from [21]. This database consists of 253 images. The proposed methodology is validated by analyzing the accuracy and loss of the brain tumor segmentation. The proposed methodology is utilized to segment the lung in addition to brain tumor from the MRI images.

Table 1: Implementation values

S. No	Technique	Parameters	Value
1	Proposed Method	Number of Decision Variables	5
2		Number of Populations	50
3		Upper bound	10
4		Lower bound	-10
5		Iteration	100

The confusion matrix is formulated related to the subsequent constraints,

- ❖ A brain tumour is segmented as a corrected condition named True Positive (TP).
- ❖ A brain tumour is not segmented, as not corrected which is defined True Negative (TN).
- ❖ A brain tumour is not segmented that is named False Positive (FP).
- ❖ A brain tumour is segmented as not corrected which is defined as False Negative (FN).

Based on the progress of confusion matrix terms, the proposed methodology is evaluated by performance metrics which are formulated as follows,

With the consideration of the confusion matrix formulation, the projected technique is computed by presentation metrices that are presented as follows.

Accuracy: It can be described as a count of optimally segmented data examples from the total number of examples. The accuracy formula is formulated as follows,

$$Accuracy = \frac{TN + TP}{TN + FP + TP + FN} \qquad (24)$$

Sensitivity: It is described as the ratio of optimally segmented positive examples to complete positive examples that presented as surveys,

$$Recall = \frac{TP}{(TP + FN)} \qquad (25)$$

Specificity: It is described as the ratio of properly segmented negative examples to complete negative examples which computed based on below equations,

$$specificity = \frac{TN}{(TN + FP)} \qquad (26)$$

DSC: It is defined as similarity index which computed based on below equation,

$$DSC = 2\frac{|S \cap G|}{|S + G|} \qquad (27)$$

$$JSI = 2\frac{|S \cap G|}{|S \cup G|} \qquad (28)$$

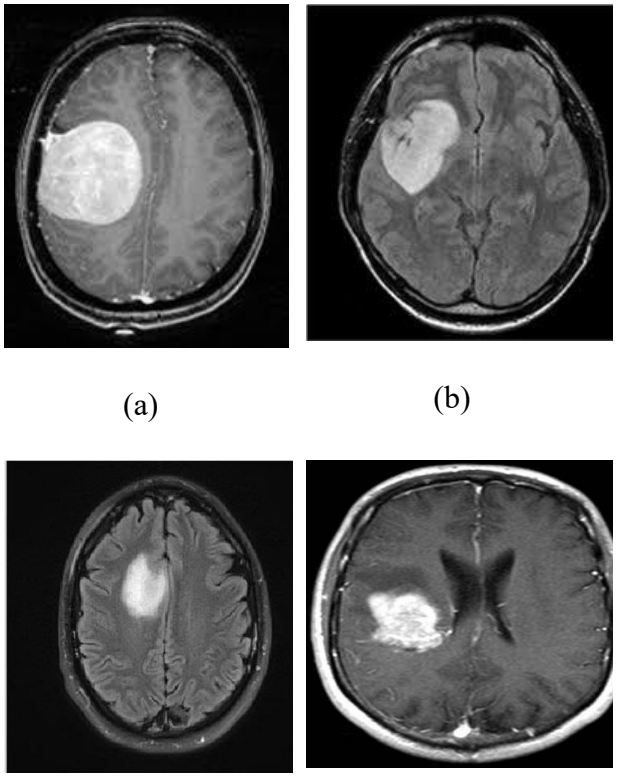

(a) (b)

(c) (d)

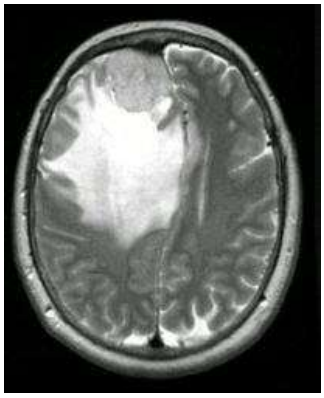

(e)

Figure 2: MRI input images

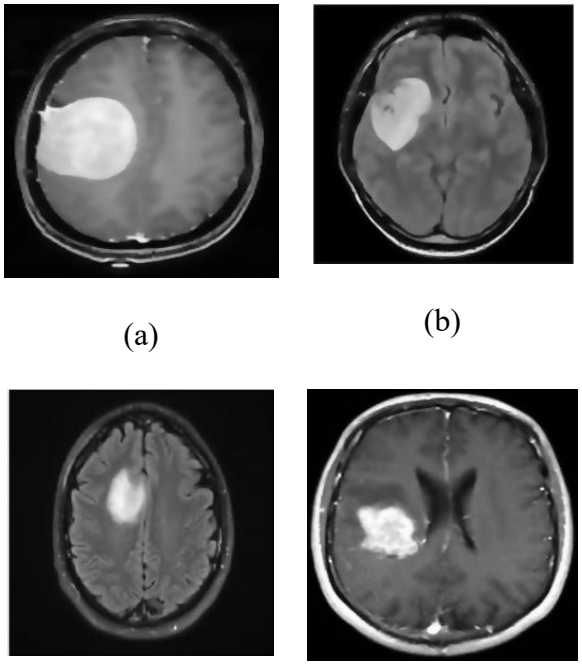

(a) (b)

(c) (d)

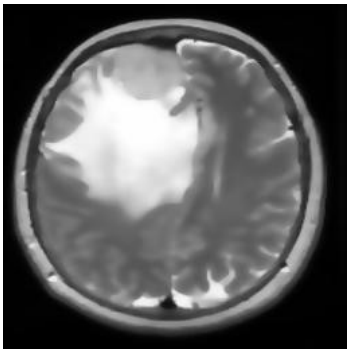

(e)

Figure 3: Pre-processing images

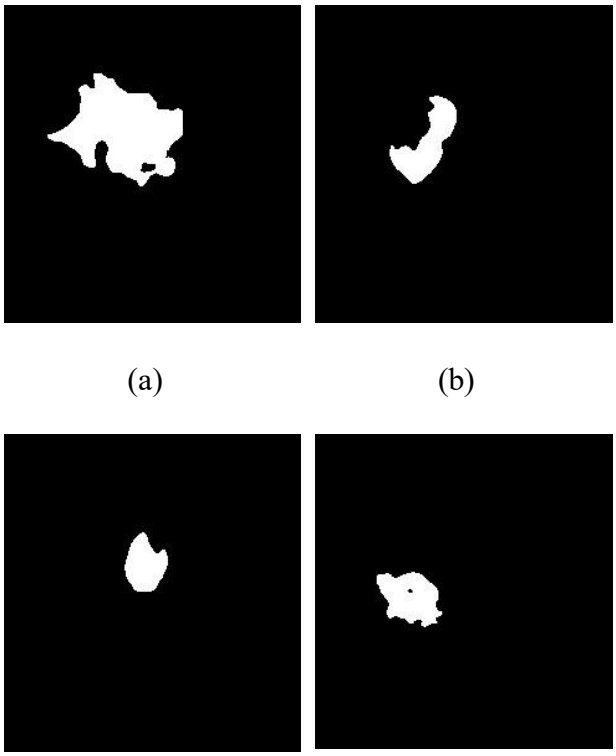

(a) (b)

(c) (d)

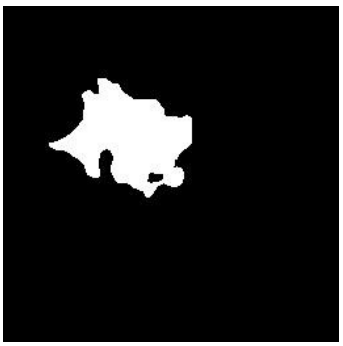

(e)

Figure 4: Segmented images

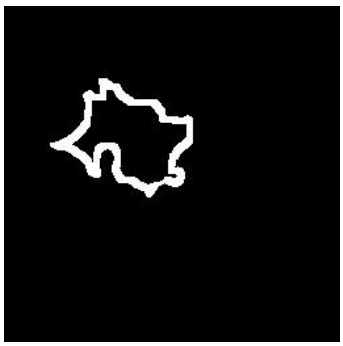

(e)

Figure 5: Tumor outlined images

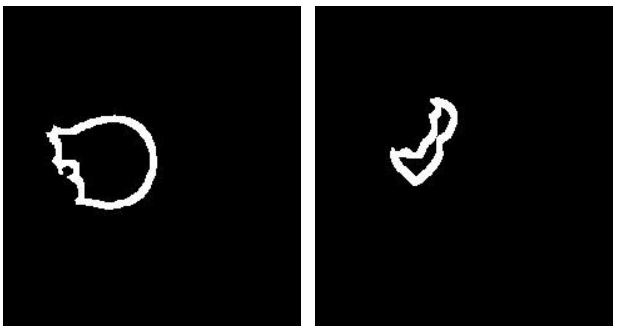

(a) (b)

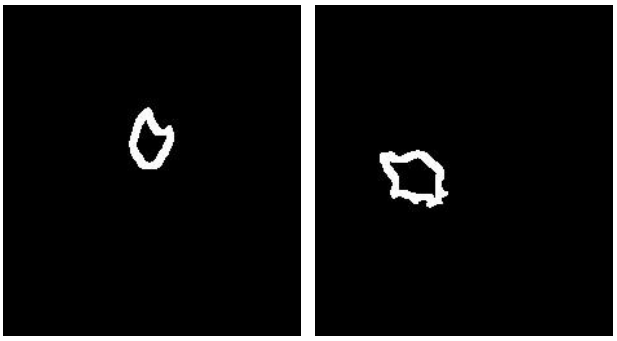

(c) (d)

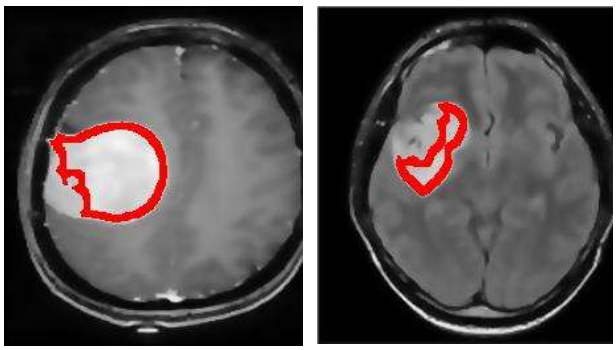

(a) (b)

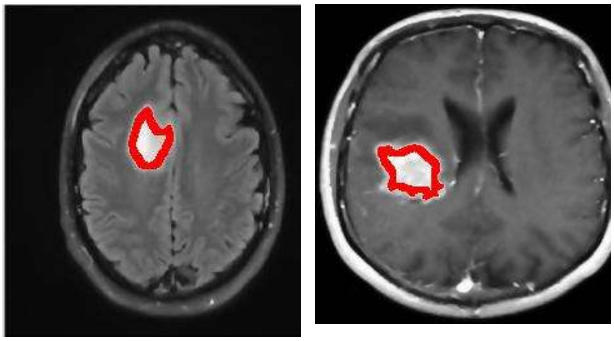

(c) (d)

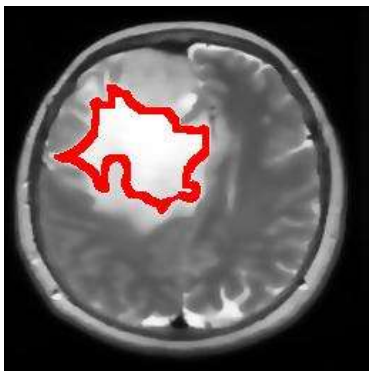

(e)

Figure 6: Tumor outlined images

The input image of MRI is illustrated in figure 2. The pre-processing and segmentation image are illustrated in figure 3 and 4. The tumour outlined images are presented in figure 5 and 6. The presentation of the projected technique is authenticated by performance metrices such as JSC, DSC, accuracy, specificity and sensitivity. To validate the presentation of projected technique is contrasted with conventional techniques like SOA-SFC in addition COA-T2FCM.

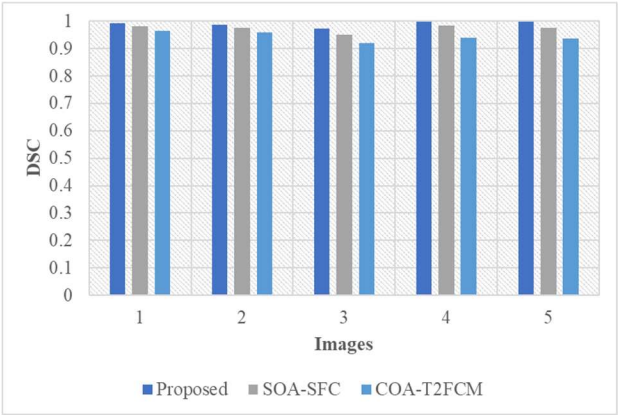

Figure 7: Analysis of DSC

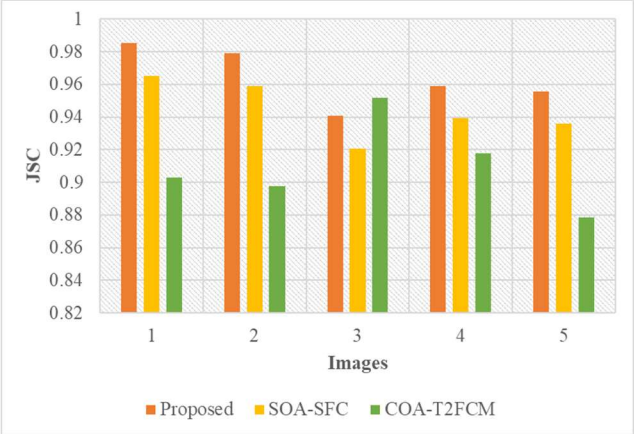

Figure 8: Analysis of JSC

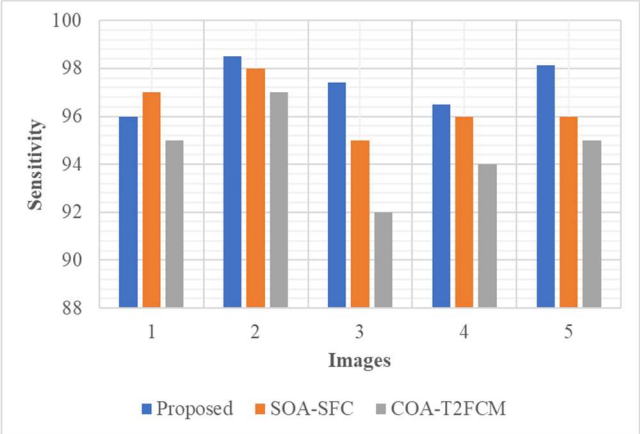

Figure 9: Analysis of sensitivity

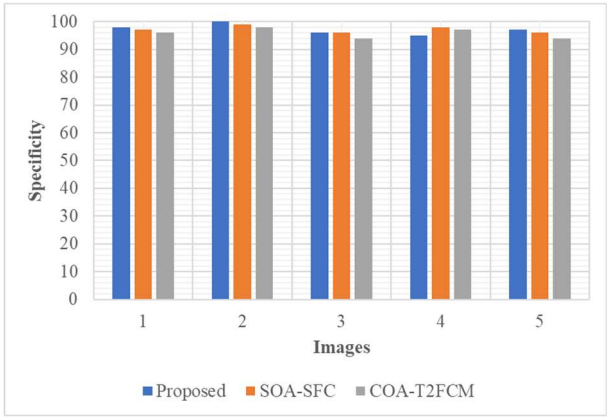

Figure 10: Analysis of specificity

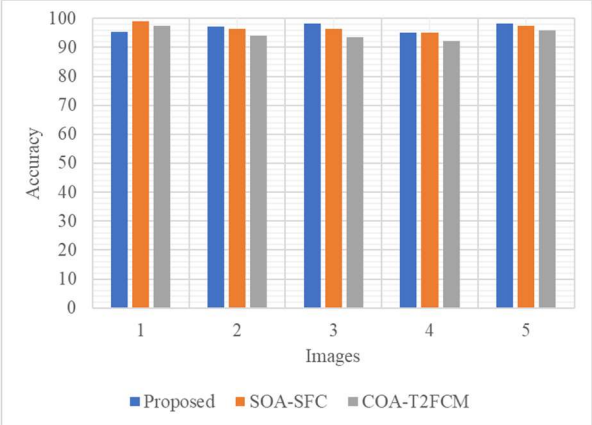

Figure 11: Analysis of accuracy

The DSC measure of the projected technique is demonstrated in figure 7. The projected technique has been achieved 0.98 DSC measure. The SOA-SFC and COA-T2FCM has been achieved 0.97 and 0.95 measure. From the analysis, we can conclude, the projected technique has been attained optimal results. The JSC measure of the projected technique is demonstrated in figure 8. The projected technique has been achieved 0.98 JSC measure. The SOA-SFC and COA-T2FCM has been achieved 0.97 and 0.91 measure. From the analysis, we can conclude, the projected technique has been attained optimal results. The sensitivity measure of the projected technique is illustrated in figure 9. The projected technique has been achieved 99 sensitivity measure. The SOA-SFC and COA-T2FCM has been achieved 97 and 95 measure. From the analysis, we can conclude, the projected technique has been achieved best results. The specificity measure of the projected technique is demonstrated in figure 10. The proposed method has been achieved 99 sensitivity measure. The SOA-SFC and COA-T2FCM has been achieved 96 and 94 measure. From the analysis, we can conclude, the projected technique has been achieved best results. The accuracy measure of the proposed method is demonstrated in figure 11. The projected technique has been achieved 99.15 accuracy measure. The SOA-SFC and COA-T2FCM has been achieved 95 and 93 measure. From the analysis, we can conclude, the projected technique has been achieved optimal outcomes.

Table 2: Proposed method comparison analysis

Image database	Method	DSC	JSC	Sensitivity	Specificity	Accuracy
Brain tumour images	Proposed	0.99	0.98515	96	98	99.4
	SOA-SFC	0.98125	0.9654	97	97	99.15
	COA-T2FCM	0.96515	0.90306	95	96	97.5
Liver tumour images	Proposed	0.97	0.9548	94	97	96.12
	SOA-SFC	0.95	0.9014	90	95	92.15
	COA-T2FCM	0.91	0.878	85	91	90.68

The projected technique is contrasted with the conventional techniques like SOA-SFC and COA-T2FCM. The two kinds of images are considered to validate the proposed methodology such as brain tumour images and liver tumour images. The performance is evaluated with the consideration of performance metrices such as DSC, JSC, sensitivity, specificity and accuracy. During segmentation process, the brain tumour segmentation is achieved 99.4 and liver tumour segmentation is achieved 96.12. Compared with the liver and brain tumour images, the brain

tumour is optimally segmented with the help of proposed methodology.

5. Conclusion

In this paper, SSA-FLS is designed for brain tumour segmentation. The proposed segmentation process is designed with the combination of FLS and SSA. In the fuzzy level set method, the efficient cluster center is chosen with the assistance of Squirrel Search Algorithm. Initially, the fuzzy level set method objective function is considered by tumour portion extraction from the MRI images. After that, SSA is utilized to optimize the cluster center and fuzzifier from the clustering method. The projected technique has been applied in the MATLAB in addition performances has been assessed. The projected technique is confirmed by performance metrices like DSC, JSI, accuracy, sensitivity, and specificity. The projected technique has been contrasted with the traditional techniques like SOA-SFC in addition COA-T2FCM. Based on the validation, the projected technique has been attained optimal outcomes in terms of JSC, DSC, sensitivity specificity and accuracy. In future, efficient method will be developed for enabling best brain tumour segmentation.

6. References

[1]. A.Selvapandian, and K. Manivannan. "Fusion based glioma brain tumor detection and segmentation using ANFIS classification." Computer methods and programs in biomedicine 166 (2018): 33-38.

[2]. Jijun Tong, Yingjie Zhao, Peng Zhang, Lingyu Chen, and Lurong Jiang. "MRI brain tumor segmentation based on texture features and kernel sparse coding." Biomedical Signal Processing and Control 47 (2019): 387-392.

[3]. Eser Sert, Fatih Özyurt, and Akif Doğantekin. "A new approach for brain tumor diagnosis system: Single image super resolution based maximum fuzzy entropy segmentation and convolutional neural network." Medical hypotheses 133 (2019): 109413.

[4]. Geethu Mohan, and M. Monica Subashini. "MRI based medical image analysis: Survey on brain tumor grade classification." Biomedical Signal Processing and Control 39 (2018): 139-161.

[5]. Shengcong Chen, Changxing Ding, and Minfeng Liu. "Dual-force convolutional neural networks for accurate brain tumor segmentation." Pattern Recognition 88 (2019): 90-100.

[6]. Fatih Özyurt, Eser Sert, Engin Avci, and Esin Dogantekin. "Brain tumor detection based on Convolutional Neural Network with neutrosophic expert maximum fuzzy sure entropy." Measurement 147 (2019): 106830.

[7]. Mohamed Akil, Rachida Saouli, and Rostom Kachouri. "Fully automatic brain tumor segmentation with deep learning-based selective attention using overlapping patches and multi-class weighted cross-entropy." Medical image analysis 63 (2020): 101692.

[8]. Abdelaziz Essadike, Elhoussaine Ouabida, and Abdenbi Bouzid. "Brain tumor segmentation with Vander Lugt correlator based active contour."

Computer methods and programs in biomedicine 160 (2018): 103-117.

[9]. Khai Yin Lim, and Rajeswari Mandava. "A multi-phase semi-automatic approach for multisequence brain tumor image segmentation." Expert Systems with Applications 112 (2018): 288-300.

[10]. Ilunga–Mbuyamba, Elisee, Juan Gabriel Avina–Jonathan Cepeda–Negrete Cervantes, Mario Alberto Ibarra–Manzano, and Claire Chalopin. "Automatic selection of localized region-based active contour models using image content analysis applied to brain tumor segmentation." Computers in biology and medicine 91 (2017): 69-79.

[11]. Mohammadreza Soltaninejad, Guang Yang, Tryphon Lambrou, Nigel Allinson, Timothy L. Jones, Thomas R. Barrick, Franklyn A. Howe, and Xujiong Ye. "Supervised learning based multimodal MRI brain tumour segmentation using texture features from supervoxels." Computer methods and programs in biomedicine 157 (2018): 69-84.

[12]. Adel Kermi, Khaled Andjouh, and Ferhat Zidane. "Fully automated brain tumour segmentation system in 3D-MRI using symmetry analysis of brain and level sets." IET Image Processing 12, no. 11 (2018): 1964-1971.

[13]. Marco Domenico Cirillo, David Abramian, and Anders Eklund. "Vox2Vox: 3D-GAN for brain tumour segmentation." arXiv preprint arXiv:2003.13653 (2020).

[14]. Mahnoor Ali, Syed Omer Gilani, Asim Waris, Kashan Zafar, and Mohsin Jamil. "Brain Tumour Image Segmentation Using Deep Networks." IEEE Access 8 (2020): 153589-153598.

[15]. Abhisha Mano, and Swaminathan Anand. "Method of multi-region tumour segmentation in brain MRI images using grid-based segmentation and weighted bee swarm optimisation." IET Image Processing 14, no. 12 (2020): 2901-2910.

[16]. Rehman, Zaka Ur, Syed S. Naqvi, Tariq M. Khan, Khan Muhammad A, and Tariq Bashir. "Fully automated multi-parametric brain tumour segmentation using superpixel based classification." Expert systems with applications 118 (2019): 598-613.

[17]. R.Radha, and R. Gopalakrishnan. "A medical analytical system using intelligent fuzzy level set brain image segmentation based on improved quantum particle swarm optimization." Microprocessors and Microsystems 79 (2020): 103283.

[18]. Bing Nan Li, Chee Kong Chui, Stephen Chang, and Sim Heng Ong. "Integrating spatial fuzzy clustering with level set methods for automated medical image segmentation." Computers in biology and medicine 41, no. 1 (2011): 1-10.

[19]. Mohit Jain, Vijander Singh, and Asha Rani. "A novel nature-inspired algorithm for optimization: Squirrel search algorithm." Swarm and evolutionary computation 44 (2019): 148-175.

[20]. Tongyi Zheng, and Weili Luo. "An improved squirrel search algorithm for optimization." Complexity 2019 (2019).

[21]. https://www.kaggle.com/navoneel/brain-mri-images-for-brain-tumor-detection